Available online at www.sciencedirect.com
ScienceDirect
Theoretical and Applied Fracture Mechanics 49 (2008) 51–60
theoretical and applied fracture mechanics
www.elsevier.com/locate/tafmec

Multi-scale modeling of tensile behavior of carbon nanotube-reinforced composites

K.I. Tserpes [a,*], P. Papanikos [b], G. Labeas [a], Sp.G. Pantelakis [a]

[a] *Laboratory of Technology and Strength of Materials, Department of Mechanical Engineering and Aeronautics, University of Patras, Patras 26500, Greece*
[b] *Department of Product and Systems Design Engineering, University of the Aegean, Ermoupolis, Syros 84100, Greece*

Available online 1 November 2007

Abstract

A multi-scale representative volume element (RVE) for modeling the tensile behavior of carbon nanotube-reinforced composites is proposed. The RVE integrates nanomechanics and continuum mechanics, thus bridging the length scales from the nano- through the mesoscale. A progressive fracture model based on the modified Morse interatomic potential is used for simulating the behavior of the isolated carbon nanotubes and the FE method for modeling the matrix and building the RVE. Between the nanotube and the matrix a perfect bonding is assumed until the interfacial shear stress exceeds the corresponding strength. Then, nanotube/matrix debonding is simulated by prohibiting load transfer in the debonded region. Using the RVE, a unidirectional nanotube/polymer composite was modeled and the results were compared with corresponding rule-of-mixtures predictions. A significant enhancement in the stiffness of the polymer owing to the adding of the nanotubes is predicted. The effect of interfacial shear strength on the tensile behavior of the nanocomposite was also studied. Stiffness is found to be unaffected while tensile strength to significantly decrease with decreasing the interfacial shear strength.

Keywords: Carbon nanotubes; Finite element analysis; Multi-scale analysis; Representative volume element; Composites

1. Introduction

Carbon nanotubes are fullerene-related structures discovered by Iijima [1]. They can be visualized as graphene sheets rolled into hollow cylinders composed of hexagonal carbon rings. Schematic representations of the graphene and nanotube are shown in Fig. 1. The nanotube structure is described in terms of a chiral vector defined by the pair of indices (n,m). According to the values of the indices, three nanotube types arise; namely, the *armchair* (n,n), the *zigzag* $(n,0)$ and the *chiral* (n,m) carbon nanotubes. Fig. 2 shows the armchair and zigzag patterns.

As the hexagonal pattern is repeated periodically, it leads to binding of each carbon atom to three neighboring atoms via covalent bonds. This covalent bond is one of the strongest chemical bonds in nature. Thus, it was expected to lend impressive mechanical properties to carbon nanotubes. Indeed, it has been experimentally and theoretically

* Corresponding author. Tel./fax: +30 2610 991027.
E-mail address: kit2005@mech.upatras.gr (K.I. Tserpes).

0167-8442/$ - see front matter © 2007 Elsevier Ltd. All rights reserved.
doi:10.1016/j.tafmec.2007.10.004

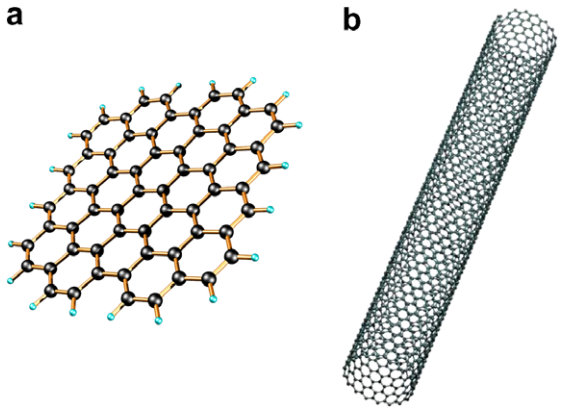

Fig. 1. Schematic representations of (a) graphene and (b) carbon nanotube.

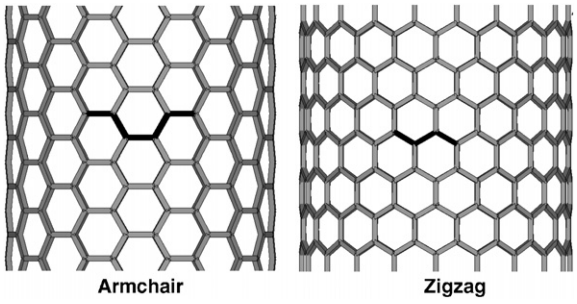

Fig. 2. Armchair and zigzag nanotube patterns.

confirmed by several studies reported in the last decade that carbon nanotubes possess extraordinary mechanical properties (elastic modulus higher than 1 TPa, tensile strength in the range of 150 GPa, elastic strain up to 5% and failure strain up to 20%).

Combining extraordinary mechanical properties and fiber-like structure, carbon nanotubes offer unique potential for reinforcing polymers either as replacements of conventional fibers or as fillers to enhance the properties of the existed advanced composites. Qian et al. [2] have demonstrated that with only 1% (by weight) of carbon nanotubes added in a matrix material, the stiffness of a resulting composite film can increase between 36% and 42% and the tensile strength by 25%. Recently, Yokozeki et al. [3] observed a clear retardation in matrix cracking onset and accumulation in composite laminates filled with carbon nanotubes.

Before establishing carbon nanotubes as mechanical reinforcements, many aspects remain to be addressed. The most important of them is to determine the bulk mechanical properties of carbon nanotube-reinforced composites; initially by assuming pristine aligned and uniformly dispersed nanotubes and afterwards, by considering possible defects in nanotube's structure, random orientation and non-uniform dispersion of reinforcing nanotubes. At present, since experimentation at the nanoscale is still evolving, the only available tool for accomplishing this task is modeling. However, due to the enormous differences in scales involved in the correlation of macroscopic properties (10^{-3}–10^{0} m) with the physical mechanisms of the nanotubes (10^{-9} m), different modeling levels need to be integrated. This can be achieved only by multi-scale approaches combining atomistic with continuum methods. So far, very few research efforts have been placed in this field. In the following paragraph, a brief description of the most representative works is given.

Li and Chou [4] reported a multi-scale modeling of the compressive behavior of carbon nanotube/polymer composites. They modeled the nanotube at the atomistic scale and analyzed the matrix deformation using the continuum FE method. The van der Waals interactions between carbon atoms and the finite element nodes of the matrix were simulated using truss rods. Computed results are in the form stress contours in the polymer matrix as well as variation of buckling force with regard to nanotube diameter and length. The approach of Li and Chou [4] is much localized and although may give very useful information regarding the interfacial load transfer between the nanotube and the matrix cannot be used for simulating the behavior of nanocomposites. Shi et al. [5] presented a hybrid atomistic/continuum mechanics method to study the deformation and fracture behavior of carbon nanotubes embedded in composites. The method is based on a representative unit cell divided into three distinct regions analyzed using an atomistic potential, a continuum method based on the Cachy–Born rule and a micromechanics method, respectively. Reported results are in the form of defect nucleation within the nanotube. The behavior of the unit cell was not examined. Odegard and coworkers [6,7] developed an equivalent-continuum modeling method for simulating large amorphous organic-based materials such as polymers, carbon nanotubes and polymer nanocomposites. This method consists of three steps; namely, the establishment of an representative volume element (RVE) of the molecular and effective-continuum model, the establishment of a constitutive relationship for the effective-continuum model

and the equation of the potential energies of deformation for identical boundary conditions. Contrary to the previous two approaches, the researchers have computed the effective elastic moduli of nanocomposites as functions of specific reinforcement characteristics. The main drawback of the equivalent-continuum method is the involvement of complicated analyses part of which may be needed to reproduce if specific features of the materials change.

From the above short overview, it is obvious that there is still a need for developing flexible multi-scale approaches that will efficiently consider the nanotube behavior at the nanoscale being at the same time able to model carbon nanotube-reinforced composites at the meso- or the microscale. In this paper, an attempt is made to develop such approach.

2. The multi-scale RVE

The proposed multi-scale approach is based on a multi-scale FE-based RVE, which is used as a building block to assemble the composite. The RVE is synthesized in two distinct steps; initially, the behavior of the isolated nanotube is simulated and then, the nanotube is inserted into the matrix to form the RVE. The synthesis of the RVE is shown in Fig. 3. Each of the steps is described in the following sections.

2.1. Behavior of isolated carbon nanotubes

In all cases where continuum methods have been used to analyze carbon nanotubes embedded in an elastic medium, a linear behavior of the reinforcements has been assumed. This assumption leads to accurate predictions only in cases where very small nanotube deformations take place. Therefore, all these methods cannot be used for modeling the mechanical behavior of the composites. In the present work, the tensile behavior of the isolated armchair and zigzag carbon nanotubes is simulated using the progressive fracture model developed in Ref. [8]. The concept of the model is based on the assumption that carbon nanotubes, when loaded, behave like space-frame structures. The bonds between carbon atoms are considered as load-carrying members while carbon atoms as joints of the members. The FE method is used to analyze the nanotube structure and the modified Morse interatomic potential [9] to describe the non-linear behavior of the C–C bonds (see Fig. 4).

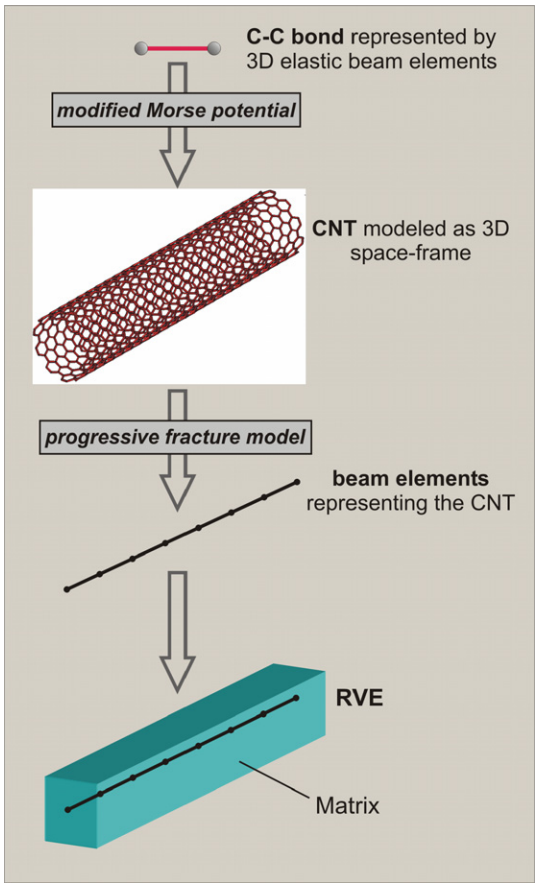

Fig. 3. Synthesis of the RVE.

2.1.1. The modified Morse potential

There are two types of interatomic potentials: pairwise and many-body. The major difference between them lies in the consideration of non-bonded interactions by many-body potentials. In general, many-body potentials are in advantage over pairwise ones especially in cases where the molecular systems sustain large deformations. In such cases, large deviations of the atoms from the equilibrium occur, imposing multiple large non-bonded interactions with their nearest neighbors, which must be taken into account. However, for

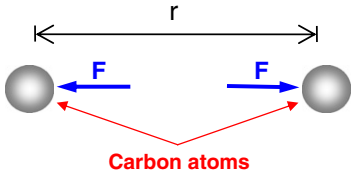

Fig. 4. Interaction between C–C bonds.

restricting the pair potential to nearest neighbors, many-body potentials introduce a cut-off function, which has found to cause strange features in the resulted force–strain curve. Belytschko et al. [9] found that in the Brenner many-body potential [10] the cut-off function causes a dramatic increase in the interatomic force (like a camelback) at the inflection point, which affects fracture behavior of the bond, and consequently of the nanotube, even when it is shifted to 100% strain.

The decision to use the modified Morse potential in the present work was strongly enforced by its simplicity over many-body potentials and its adaptability with the FE method. To date, the modified Morse potential has been adequately applied in a number of cases where there are large deviations from equilibrium due to the presence of large strains. Belytschko et al. [9] applied the potential for simulating fracture of carbon nanotubes subjected to axial tension, Xiao et al. [11] for predicting the mechanical properties of carbon nanotubes and Sun and Zhao [12] for predicting stiffness and strength of single-walled carbon nanotubes.

According to the modified Morse potential, the potential energy of the nanotube system is expressed as

$$E = E_{\text{stretch}} + E_{\text{angle}}, \tag{1}$$

$$E_{\text{stretch}} = D_e\{1 - e^{-\beta(r-r_0)}]^2 - 1\}, \tag{2}$$

$$E_{\text{angle}} = \frac{1}{2}k_\theta(\theta-\theta_0)^2[1 + k_{\text{sextic}}(\theta-\theta_0)^4] \tag{3}$$

where E_{stretch} is the bond energy due to bond stretching and E_{bend} the bond energy due to bond angle-bending, r is the current bond length and θ is the current angle of the adjacent bond. The parameters of the potential are [9]

$$r_0 = 1.421\times10^{-10}\ \text{m},\quad D_e = 6.03105\times10^{-19}\ \text{N m},$$
$$\beta = 2.625\times10^{10}\ \text{m}^{-1},\quad \theta_0 = 2.094\ \text{rad},$$
$$k_\theta = 0.9\times10^{-18}\ \text{N m/rad}^2, k_{\text{sextic}} = 0.754\ \text{rad}^{-4}$$

This is the usual Morse potential except that the bond angle-bending energy has been added and the parameters have been slightly modified by Belytschko et al. [9] so that it corresponds with the Brenner potential [10] for strains below 10%. As bond stretching dominates nanotube fracture and the effect of angle-bending potential is very small, only the bond stretching potential is considered.

By differentiating Eq. (2), the stretching force of atomic bonds is obtained in the molecular force-field as

$$F = 2\beta D_e(1 - e^{-\beta(r-r_0)})e^{-\beta(r-r_0)} \tag{4}$$

Fig. 5 plots the relationship between force F and bond strain ε for the C–C bonds. The strain of the bond is defined by $\varepsilon_b = (r - r_0)/r_0$. As may be seen, the force–strain relation is highly non-linear at the attraction region especially at large strains. The inflection point (peak force) occurs at 19% strain. The repulsive force ($\varepsilon_b < 0$) increases rapidly as the bond length shortens from the equilibrium length with less non-linearity than the attractive force.

2.1.2. FE analysis of carbon nanotubes

In the FE model, the exact atomic structure of the nanotube is modeled. The C–C bond is represented using 3D elastic beam elements (ANSYS BEAM4 elements [13]) with solid circular cross-sectional area. The non-linear behavior of the C–C bonds, as described by the interatomic potential, is assigned to the beam elements using the stepwise procedure of progressive fracture modeling briefly described in the following lines. Initially, the stiffness of the beam elements is evaluated from the initial slope of the force–strain curve of the modified Morse potential (Fig. 5) using the element's cross-sectional area $A_b = \pi D_b^2/4$ (D_b is the bond diameter corresponding to nanotube thickness t_n which is equal to 0.34 nm). The initial stiffness is 1.33 TPa. The nanotube is loaded by an incremental displacement at one of each ends with the other end being fully constrained (see Fig. 6). Zero transverse displacement is applied to the loading end in order to prevent nanotube buckling at high loads. At each load step, the stiffness of each element is set equal to $F/A_b\varepsilon_b$, where ε_b is the

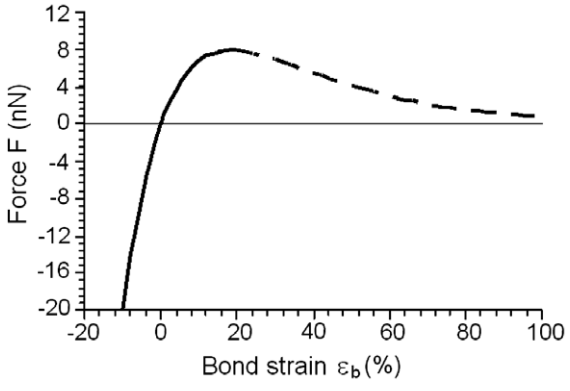

Fig. 5. The force–strain curve of the modified Morse potential.

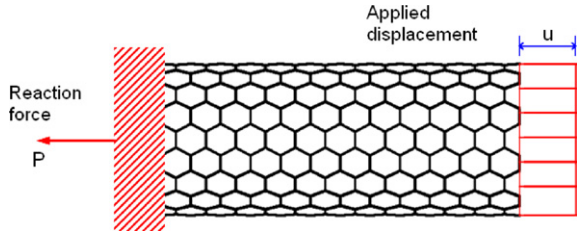

Fig. 6. Nanotube under tension.

axial strain of the element as evaluated from the FE model and F is the interatomic force computed from Eq. (4). This calculation of stiffness is accomplished until the inflection strain of the interatomic potential. When the axial strain ε_b of a bond reaches the inflection strain (19%), its stiffness is suddenly degraded (10^{-6} of the initial value) and the bond is disabled from carrying load.

The accuracy of progressive fracture modeling procedure depends on the number of load steps chosen. In order to maximize the accuracy of computational results, in each case, the displacement increment was chosen from convergence tests in which the convergence criterion was set equal to 2% of the failure stress. Thereby, if between two sequential displacement increments a difference smaller than the 2% was achieved in the computed failure stress, the larger displacement increment was finally adopted for the analysis.

2.1.3. 'Generalized' stress–strain curves of carbon nanotubes

From the first few analyses conducted it was found that

$$E_n A_n \sim D_n \tag{5}$$

where $E_n A_n$ is nanotube's tensile rigidity given by $E_n A_n = P/\varepsilon_n$; P is the reaction force, A_n is the nanotube's cross-sectional area and D_n is the nanotube mean diameter. The above analogy is demonstrated in Fig. 7a and b for two sets of armchair and zigzag nanotubes. Since A_n is a linear relation of $D_n (A_n = \pi D_n t_n)$, the stress is kept constant. Therefore, for each type of nanotubes the tensile stress–strain curves are the same. The 'generalized' stress–strain curves of the armchair and zigzag nanotubes are shown in Fig. 8. In these curves, the extraordinary mechanical properties of carbon nanotubes are revealed.

By fitting the data of the curves using third-order polynomials, the following relations between the nanotube stress and strain are obtained

$$\sigma_n = 5958.5\varepsilon_n^3 - 4769.4\varepsilon_n^2 + 1334.7\varepsilon_n \quad \text{(armchair nanotubes)} \tag{6}$$

$$\sigma_n = 2909.8\varepsilon_n^3 - 4995.6\varepsilon_n^2 + 1364.9\varepsilon_n \quad \text{(zigzag nanotubes)} \tag{7}$$

From Eqs. (6) and (7), the stiffness of the nanotubes is simply derived as a function of strain

$$E_n = 5958.5\varepsilon_n^2 - 4769.4\varepsilon_n + 1334.7 \quad \text{(armchair nanotubes)} \tag{8}$$

$$E_n = 2909.8\varepsilon_n^2 - 4995.6\varepsilon_n + 1364.9 \quad \text{(zigzag nanotubes)} \tag{9}$$

Using Eqs. (8) and (9) in a similar manner Eq. (4) was used to simulate the behavior of the C–C

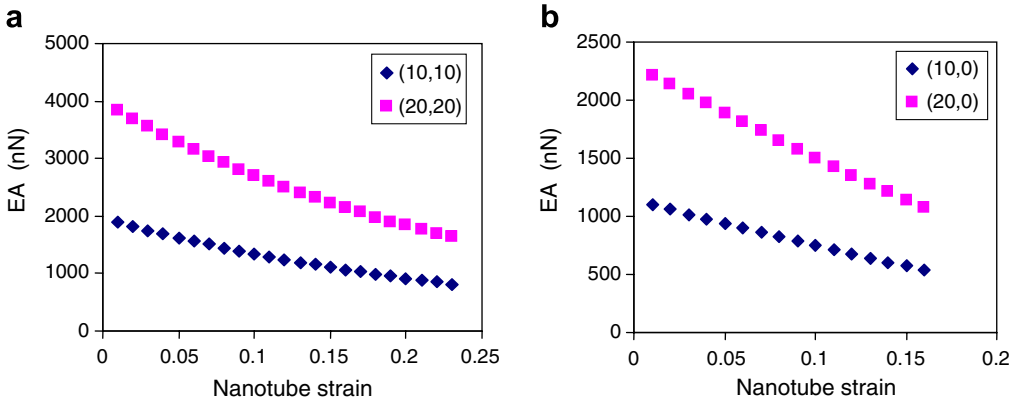

Fig. 7. Nanotube's tensile rigidity as a function of strain for (a) armchair and (b) zigzag nanotubes.

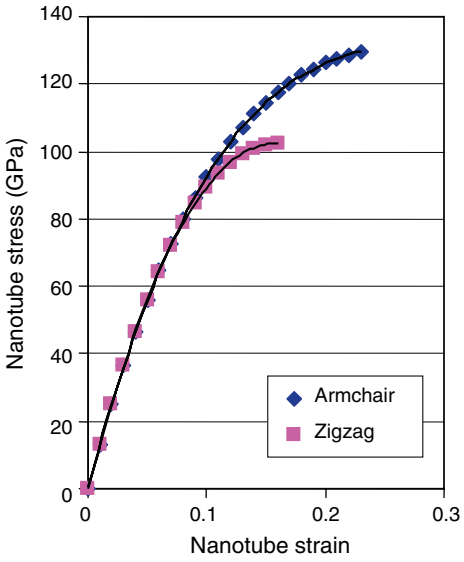

Fig. 8. Generalized stress–strain curves for the armchair and zigzag nanotubes.

bonds, the tensile behavior of nanotubes is modeled in terms of varying stiffness.

2.2. Building the RVE

The RVE is a rectangular solid whose entire volume is taken up by the matrix. In order to reduce the computational effort and make the RVE more versatile, instead of modeling the nanotube as a solid or hollow cylinder, it is superimposed to the matrix as can be seen in Fig. 9a. 3D isotropic solid elements are used for modeling the matrix while the nanotube is represented by 3D elastic beam elements created by binding the nodes of the matrix. As in the present study implementation was done in the ANSYS commercial FE code, the 3D SOLID45 and BEAM4 elements were, respectively, used. For the beam elements, a hollow circular cross-sectional area was adopted. The behavior of the beam elements is described by means of Eqs. (8) and (9).

2.2.1. Verification of the RVE and effect of mesh density

Since RVE is destined to be used as a building block for modeling carbon nanotube-reinforced composites, it is very important to comprise a coarse mesh in order to reduce the computational effort required for the analysis of the assembled composite. A parametric study has been conducted to assess the effect of mesh density and select the optimum mesh giving accurate numerical results in the minimum computational time. As a reference for the study, the effective axial modulus (1.3255) evaluated by Chen and Liu [14] for a similar RVE was used. The data of the comparison case are

Nanotube stiffness:

$E_n = 1$ TPa, $\nu = 0.3$ Matrix: $E_m = 0.1$ TPa, $\nu = 0.3$

Nanotube volume fraction:

$V_{fNT} = 3.617\%$ Nanotube thickness: $t_n = 0.4$ nm

Table 1 summarizes the computed results predicted using a conventional personal computer Pentium 4 CPU 3.2 GHz for different mesh densities. The values of the effective transverse modulus E_y have been also added for thoroughness of the study. The RVE was loaded in axial tension and its effective axial modulus was computed as

Table 1
RVE's effective elastic moduli for different mesh densities

Number of elements	E_x/E_m	E_y/E_m	Elapsed time (sec)
259400	1.329	1.050	13200
32500	1.329	1.051	145
5050	1.329	1.051	12
425	1.330	1.056	2
30	1.337	1.073	2

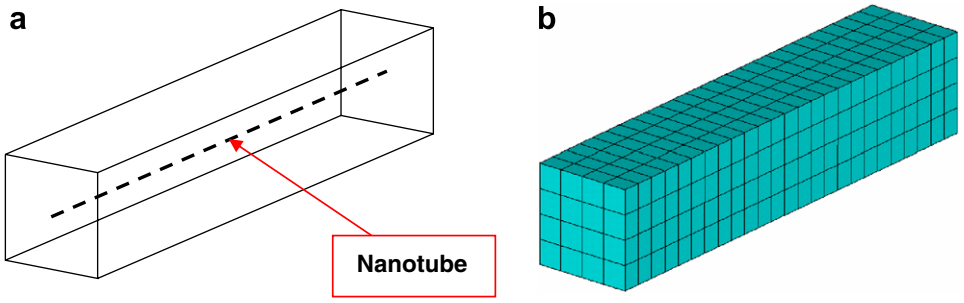

Fig. 9. (a) Reinforcement and (b) FE mesh of the RVE.

$$E_x = \frac{F_x L}{u_x A} \tag{10}$$

where u_x is the displacement applied at one end, F_x is the total reaction force at the opposite end, L is the length of the RVE and A is the sum of the nanotube and matrix areas.

Between the predicted value of the effective axial stiffness (1.329) and the value reported by Chen and Liu [14] (1.326) a very good agreement is obtained, thus verifying the RVE proposed herein. Regarding the effect of mesh density on the computed effective elastic moduli, the results show that it is minor and only in coarse meshes comprising less than 100 elements the predicted values start to diverge. Based on the above, we conclude that the mesh comprising 425 elements (see Fig. 9b) can be safely adopted. Note that the choice of Chen and Liu [14] to model the carbon nanotube as a hollow cylinder resulted in a mesh comprising almost 4500 elements, which is more than ten times the current mesh.

2.3. Nanotube/matrix debonding

Fundamental to the reinforcing effectiveness are the interfacial characteristics between the nanotube and the matrix. Upon this issue, a considerable number of works have been reported lately. However, in all cases the interfacial characteristics have been studied independently without being associated with the mechanical properties of the composite. In the RVE proposed herein, simulation of nanotube/matrix debonding is incorporated. As carbon nanotubes are represented by beam elements, the interfacial shear stress cannot be computed directly. To overcome this obstacle, we employed a shear-lag approach described in the following paragraph.

Consider one of the beam elements representing the nanotube in the RVE. The element lies between nodes 1 and 2 and is under axial tension. Its

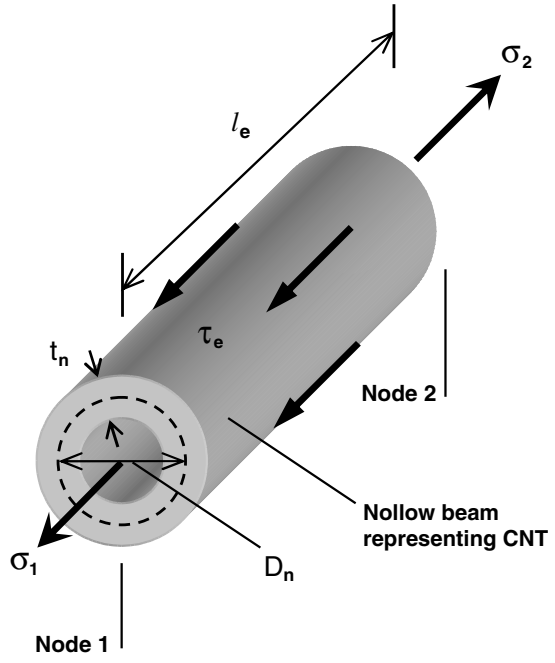

Fig. 10. The free-body diagram of the beam representing the nanotube.

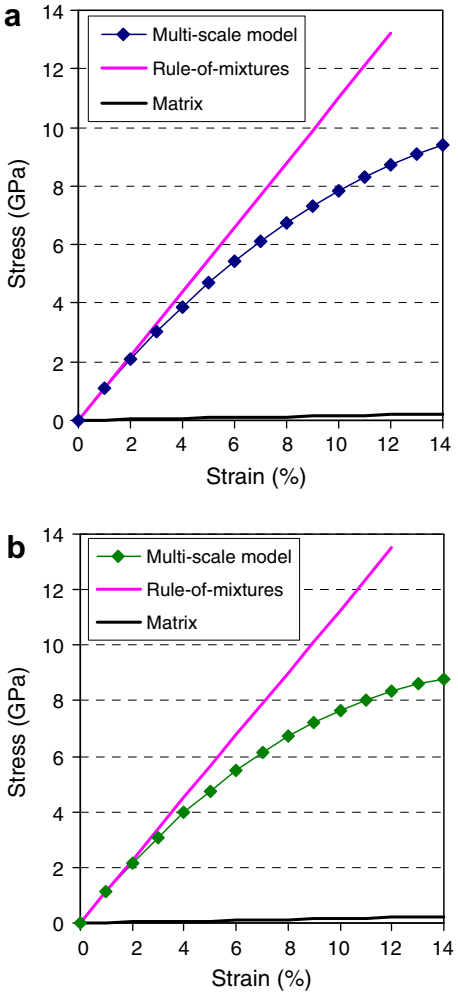

Fig. 11. Comparison between the predicted tensile stress–strain curves for the nanocomposite specimens and the results from the rule-of-mixtures: (a) armchair nanotube reinforcement and (b) zigzag nanotube reinforcement.

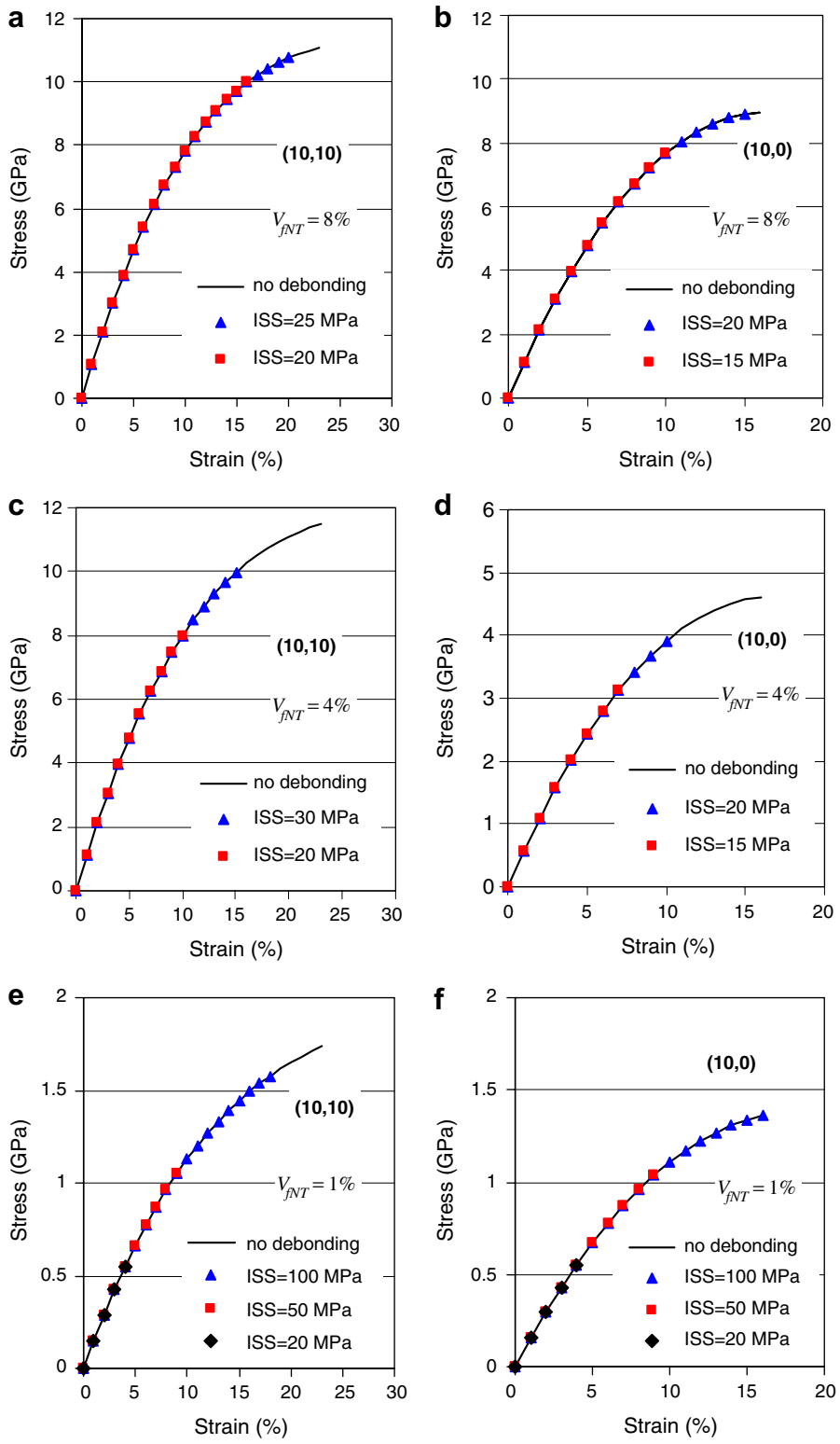

Fig. 12. Predicted tensile stress–strain curves for the nanocomposite for various interfacial shear strengths and nanotube volume fractions. The reinforcing nanotubes and values of V_{fNT} are indicated in the graphs.

free-body diagram is shown in Fig. 10. From the FE analysis, the normal stresses σ_1 and σ_2 at nodes 1 and 2, respectively, are computed. If we assume constant shear stress τ_e along the element, then the equilibrium imposes

$$|\sigma_1 - \sigma_2|A_n = \tau_e \pi (D_n + t_n) l_e \quad (11)$$

where $D_n + t_n$ is the outer nanotube diameter (beam) and l_e is the beam's length. From Eq. (11) we solve for τ_e and compare this value to the interfacial shear strength (ISS). If $\tau_e \geqslant$ ISS, the interface has failed leading to load-carrying disability of the specific element, which is modeled by assigning to it a very small stiffness. The above procedure is repeated at each load step.

3. Nanocomposite under tension

A unidirectional nanotube/polymer composite was modeled by stacking the RVE in a $3 \times 3 \times 3$ figure. The armchair (10, 10) and zigzag (10, 0) nanotubes spanning the length of the matrix were used as reinforcements. The nanotube volume fraction is 8%. The nanocomposite specimen was subjected to axial tension by fully constraining the nodes of the one end and applying an incremental displacement at the nodes of other.

For a composite under uniaxial loading, the dependence of elastic modulus on the nanotube volume fraction can be estimated by the rule-of-mixtures. Under constant strain conditions, the longitudinal elastic modulus of the composite E_C is given by

$$E_C = E_{NT} V_{fNT} + E_M V_{fM} \quad (12)$$

where E_{NT} and E_M are the longitudinal elastic moduli of the nanotube and the matrix, respectively, and V_{fM} are the matrix volume fraction. For $V_{fNT} = 8\%$, $E_{NT} = 1.33$ TPa and $E_M = 2$ GPa we get $E_C = 108.24$ GPa.

Fig. 11a and b compares the tensile stress–strain curves predicted by the multi-scale model with the results from the rule-of mixtures analysis. A line indicating the stiffness of the polymer was added for comparison reasons. In these initial analyses, no debonding between the nanotube and the polymer was considered. As can be seen, the addition of carbon nanotubes enhanced significantly the stiffness of the matrix. At low strains, the predicted stress–strain curves coincide with the linear behavior given by the rule-of-mixtures. The deviation observed at larger strains is due to the non-linear behavior of carbon nanotubes.

3.1. Effect of interfacial shear strength

The property of nanotube/polymer interface that has been studied the most is the interfacial shear strength (ISS). The studies reported to date agree that the ISS is high but give scattered values. Wagner et al. [15] inferred from fragmentation tests that the stress transfer ability of nanotube/polymer interface could be in the order of 500 MPa, an order of magnitude higher than the one of micro carbon fiber composites. More recently, Cooper et al. [16] found from pullout experiments that the ISS between a multi-walled carbon nanotube and epoxy ranged from 35 to 375 MPa. Given the uncertainty of ISS value, a parametric study was conducted in order to assess its effect on the tensile behavior of the nanocomposite.

Fig. 12a–f shows the effect of ISS on the tensile behavior of nanocomposites in relation with the nanotube volume fraction. The values of ISS considered ranged from 15 to 100 MPa while the values of V_{fNT} from 1% to 8%. Whereas the strength decreases significantly with decreasing the ISS, the stiffness of the nanotubes is not influenced. The comparison of the predicted strength for ISS = 20 MPa is presented in Fig. 13. For the same applied stress, the shear stress is larger for low values of V_{fNT}. This is due to the higher strain experienced by the nanotube for low values of V_{fNT}. This results in higher load transfer at the matrix/nanotube interface. Fig. 13 also shows that, for the same ISS, doubling the volume fraction leads to more than two times larger strength.

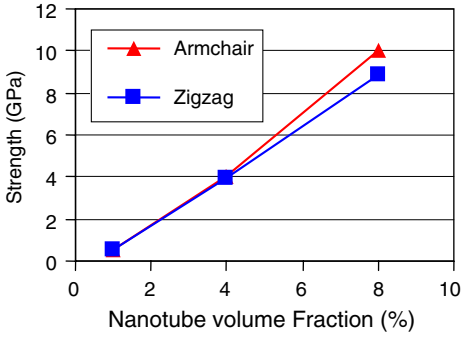

Fig. 13. Effect of nanotube volume fraction on the nanocomposite's tensile strength (ISS = 20 MPa).

4. Conclusions

The conclusions of the paper are summarized as follows:

1. A multi-scale RVE for modeling the tensile behavior of carbon nanotube-reinforced composites is proposed. The continuum FE method is employed for building the RVE and performing the analysis while data regarding the behavior of the nanotube are drawn from an atomistic interatomic potential. Incorporated in the analysis is the simulation of nanotube/matrix debonding employing an engineering mechanics approach. Thus, the investigation of the impact of interfacial failure in the mechanical properties of the composite is enabled.
2. Using the RVE, the tensile behavior of a unidirectional nanotube/polymer composite was modeled. A significant enhancement in the stiffness of the polymer owing to the addition of the nanotubes was predicted. The prediction of composite's initial stiffness was verified by the rule-of-mixtures.
3. The effect of interfacial shear strength on the tensile behavior of the composite was studied in relation with nanotube volume fraction. It was found that the stiffness is unaffected while tensile strength significantly decreases with decreasing the interfacial shear strength. A significant increase of tensile strength with increasing the nanotube volume fraction was also found.

References

[1] S. Iijima, Helical microtubules of graphitic carbon, Nature 354 (1991) 56–68.
[2] D. Qian, E. Dickey, R. Andrews, T. Rantell, Load transfer and deformation mechanisms in carbon nanotube-polystyrene composites, Applied Physics Letters 76 (20) (2000) 2868–2870.
[3] T. Yokozeki, Y. Iwahori, S. Ishiwata, Matrix cracking behaviors in carbon fiber/epoxy laminates filled with cup-stacked carbon nanotubes (CSCNTs), Composites Part A 38 (2007) 917–924.
[4] C. Li, T.-W. Chou, Multiscale modeling of compressive behavior of carbon nanotube/polymer composites, Composites Science and Technology 66 (14) (2006) 2409–2414.
[5] D. Shi, X. Feng, H. Jiang, Y.Y. Huang, K. Hwang, Multiscale analysis of fracture of carbon nanotubes embedded in composites, International Journal of Fracture 134 (2005) 369–386.
[6] G.M. Odegard, T.S. Gates, L.M. Nicholson, K.E. Wise, Equivalent continuum modeling of nano-structured materials, Composites Science and Technology 62 (2002) 1869–1880.
[7] G.M. Odegard, T.S. Gates, K.E. Wise, C. Park, E.J. Siochi, Constitutive modeling of nanotube–reinforced polymer composites, Composites Science and Technology 63 (2003) 1671–1687.
[8] K.I. Tserpes, P. Papanikos, A progressive fracture model for carbon nanotubes, Composites Part B 37 (7–8) (2006) 662–669.
[9] T. Belytschko, S. Xiao, G. Schatz, R. Ruoff, Atomistic simulations of nanotube fracture, Physical Review B 65 (25) (2002) 235430.
[10] D.W. Brenner, Empirical potential for hydrocarbons for use in simulating the chemical vapor deposition of diamond films, Physical Review B 42 (1990) 9458.
[11] J.R. Xiao, B.A. Gama, J.W. Gillespie Jr., An analytical molecular structural mechanics model for the mechanical properties of carbon nanotubes, International Journal of Solids and Structures 42 (2005) 3075–3092.
[12] X. Sun, W. Zhao, Prediction of stiffness and strength of single-walled carbon nanotubes by molecular-mechanics based finite element approach, Materials Science and Engineering 390 (2005) 366–371.
[13] ANSYS User's Manual, Version 10, Swanson Analysis Systems Inc., 2006.
[14] X.L. Chen, Y.J. Liu, Square representative volume elements for evaluating the effective material properties of carbon nanotube-based composites, Computational Materials Science 29 (2004) 1–11.
[15] H.D. Wagner, O. Lourie, Y. Feldman, R. Tenne, Stress-induced fragmentation of multiwall carbon nanotubes in a polymer matrix, Applied Physics Letters 72 (2) (1998) 188–190.
[16] C.A. Cooper, S.R. Cohen, A.H. Barber, H.D. Wagner, Detachment of nanotubes from a polymer matrix, Applied Physics Letters 81 (20) (2002) 3873–3875.